Titanomagnetites from a differentiation sequence, analcime-olivine theralite to analcime-tinguaite

By J. F. G. WILKINSON

Department of Geology, The University of New England, Armidale, New South Wales.

Summary. Six titanomagnetites from a differentiated alkaline intrusion have been studied using microscopic, chemical, and X-ray techniques. The titanomagnetites are homogeneous; with differentiation their FeO and TiO_2 contents decrease, and Fe_2O_3 increases. The titanomagnetite course of crystallization extends from close to the ulvöspinel–magnetite join, near to ulvöspinel, towards magnetite. The recalculated normative compositions of three titanomagnetites indicate that they are essentially Fe_3O_4–(γ-$FeTiO_3$)–(γ-Fe_2O_3) solid solutions. The changing chemistry of the titanomagnetites is ascribed primarily to variations in the chemistry of the magma during differentiation.

FROM the chemical petrology standpoint, the iron-titanium oxides in igneous rocks have not been accorded the attention directed to the more common igneous silicates. Some studies on these oxides from certain differentiated basic intrusions have been carried out (e.g. Vincent and Phillips, 1954; Wilkinson, 1957; Vincent, 1960); Buddington *et al.* (1955) have recognized differing trends in the TiO_2 contents of titaniferous magnetite with decreasing temperature. However, comparatively few investigations have been concerned with the behaviour of titanomagnetite[1] as the predominant iron-titanium oxide phase crystallizing from a mafic → felsic differentiation series. In any evaluation of the changing chemistry of titanomagnetite with differentiation, it is highly desirable that the parent rocks have cooled sufficiently rapidly to minimize any exsolution or sub-solidus oxidation phenomena within the titanomagnetite.

The Square Top intrusion, near Nundle, New South Wales, meets these prerequisites. This strongly differentiated intrusion, 250–300 feet thick, shows the progressive change from analcime–olivine theralite occurring at the lower intrusion levels, to analcime–tinguaite in the upper portions (table IV; fig. 3).

[1] In this paper the term 'titanomagnetite' denotes a single phase solution of TiO_2 compounds in magnetite (Buddington *et al.*, 1955; Basta, 1960).

Rock crushes (−120 mesh) were prepared initially using a Braun disk miller fitted with ceramic disks. The impure magnetic concentrates were finely ground under acetone to remove adhering silicates and then repeatedly centrifuged in warm saturated Clerici solution. Transmitted and reflected light examination of the final concentrates indicated a purity generally greater than 98 %; the most impure titanomagnetite (ST.11) contains 0·63 % SiO_2. The titanomagnetites were subsequently studied by microscopic, X-ray, and chemical techniques.

Microscopic study of the titanomagnetites

The following description deals primarily with the specimens from which the analysed titanomagnetites were separated (table I, analyses 1–6). In general the theralites and tinguaites are porphyritic in titaniferous salite and olivine (where present). In the lower theralites, the titanomagnetite grains, predominantly idiomorphic, may range up to 0·15 mm in diameter, but are generally smaller (0·05 mm). Some titanomagnetite is present as inclusions in clinopyroxene phenocrysts (up to 4 mm in diameter) and to a lesser extent in olivine (up to 2 mm); most of the titanomagnetite is confined to the felsic areas of plagioclase, alkali feldspar, nepheline and analcime (and minor natrolite and apatite). In the more differentiated theralites, some titanomagnetite grains are indented by prisms of groundmass clinopyroxene.

In the tinguaites the titanomagnetite grains increase in size (0·1 mm). As the theralites merge into the tinguaites, the amount of modal opaque oxide decreases. The upper tinguaites are porphyritic in clinopyroxene (now slightly acmitic) and nepheline; the titanomagnetite grains are larger than groundmass alkali feldspar laths. Although there is a tendency for some titanomagnetite to be marginally indented by and partly intersertal to alkali feldspar, it does not at any stage become markedly skeletal.

Reflected light examination (×1000 in oil) does not indicate any exceptional features. When studied in rock polished sections and in mounted concentrates, the titanomagnetite is homogeneous. The high TiO_2 contents of titanomagnetites ST.28, ST.20, ST.23 (all containing more than 20 % TiO_2) produces a definite brownish-pink colour in these minerals. The titanomagnetites in the upper tinguaites contain lesser amounts of TiO_2 (8–10 %) and generally show a more normal colour; some grains do show a pinkish tint. Very occasional titanomagnetite grains in polished mounted concentrates from the upper parts of the intrusion show slight marginal hematite. Minor sulphides (pyrite and chalcopyrite) are present in some rock polished sections.

TABLE I. Chemical analyses and cell dimensions of titanomagnetites from the Square Top intrusion

Analysis no.		1	2	3	4	5	6
Sample no.		ST.28	ST.20	ST.23	ST.40	ST.12	ST.11
Weight per cent.							
MO	FeO	50·13	44·64	44·23	33·31	30·57	29·74
	MgO	2·04	1·30	1·21	0·57	0·60	n.d.
	MnO	0·68	0·78	0·91	0·91	0·95	0·70
	CaO	0·16	0·09	0·63	0·22	0·19	n.d.
R_2O_3	Fe_2O_3	18·28	26·16	28·45	48·77	58·19	59·56
	Al_2O_3	2·39	3·10	0·93	tr.	0·42	tr.
TO_2	TiO_2	25·65	23·57	23·05	16·34	9·57	8·71
	SiO_2	0·20	0·25	0·49	0·26	0·38	0·63
Total		99·53	99·89	99·90	100·38	100·87	99·34
a (Å; Co$K\alpha_1$)							
	Diffractometer	8·492	8·477	8·480	8·428	8·410	8·406
	Powder photo	8·493	8·477	8·481	8·430	8·409	8·410
	Value adopted	8·493	8·477	8·481	8·429	8·410	8·408
		Numbers of ions on a basis of 32(O)					
	Fe^{2+}	12·247	10·765	10·796	8·116	7·502	7·435
	Mg	0·888	0·558	0·526	0·247	0·263	—
	Mn	0·168	0·191	0·224	0·224	0·236	0·178
	Ca	0·051	0·028	0·196	0·068	0·060	—
	Fe^{3+}	4·019	5·675	6·249	10·691	12·850	13·397
	Al	0·821	1·053	0·319	—	0·145	—
	Ti	5·634	5·110	5·059	3·579	2·112	1·957
	Si	0·058	0·073	0·144	0·075	0·111	0·189
	$\sum$ cations	23·89	23·45	23·51	23·00	23·28	23·16
Rock D.I.*		39·0	52·4	—	71·3	79·4	—

1. Titanomagnetite from analcime–olivine theralite, close to lower western contact, Square Top intrusion.
2. Titanomagnetite from leucocratic analcime–olivine theralite, on southern face, approximately 70 feet above 1.
3. Titanomagnetite from leucocratic analcime–olivine theralite, close to lower northern contact.
4. Titanomagnetite from melanocratic analcime–tinguaite, about 100 feet above lower eastern contact.

5 and 6. Titanomagnetites from analcime–tinguaites from exposed top of intrusion. (Analyses 1, 2, 5 by J. H. Pyle; analyses 3, 4, 6 by M. Chiba.)

* Differentiation index = normative Or + Ab + Ne.

Chemical and X-ray data

The chemical analyses and cell dimensions of six titanomagnetites are listed in table I. In table II these analyses have been recalculated into normative mineralogical compositions, following the method of Vincent *et al.* (1957). Titanomagnetites ST. 28 and ST. 11 (which represent the

range of composition present in the Square Top minerals) are compared with other TiO_2-bearing magnetites in table III.

The titanomagnetite compositions in numbers of ions based on 32(O) are listed in table I. In the case of titanomagnetite ST.28 (essentially a Fe_2TiO_4–Fe_3O_4 solid solution), the sum of the cations (23·89) is close

TABLE II. Normative compositions of titanomagnetites from the Square Top intrusion (100 %)

Analysis no.	1	2	3	4	5	6
Sample no.	ST.28	ST.20	ST.23	ST.40	ST.12	ST.11
Weight per cent.						
Magnetite, etc.						
$FeO.Fe_2O_3$	24·41	35·52	37·95	61·79	70·04	69·04
$MgO.Fe_2O_3$	1·60	1·60	1·60	1·59	2·18	—
$MnO.Fe_2O_3$	0·23	0·60	0·69	1·84	2·06	1·62
$CaO.Fe_2O_3$	0·22	0·11	0·65	0·43	0·43	—
$FeO.Al_2O_3$	3·66	4·87	1·39	—	0·56	—
$MgO.Al_2O_3$	0·21	0·20	0·07	—	0·01	—
$MnO.Al_2O_3$	0·05	0·09	0·03	—	0·02	—
$CaO.Al_2O_3$	0·02	0·02	0·02	—	—	—
	30·40	43·01	42·40	65·65	75·30	70·66
Ulvöspinel, etc.						
$2\ FeO.TiO_2$	61·72	36·08	38·22	—	—	—
$2\ MgO.TiO_2$	3·20	1·28	1·28	—	—	—
$2\ MnO.TiO_2$	0·89	0·67	0·89	—	—	—
$2\ CaO.TiO_2$	0·19	0·10	0·58	—	—	—
	66·00	38·13	40·97	—	—	—
Ilmenite, etc.						
$FeO.TiO_2$	3·35	17·79	15·46	29·60	17·60	17·82
$MgO.TiO_2$	0·09	0·72	0·60	0·72	0·48	—
$MnO.TiO_2$	0·05	0·30	0·30	0·74	0·59	0·45
$CaO.TiO_2$	0·01	0·05	0·27	0·27	0·14	—
	3·50	18·86	16·63	31·33	18·81	18·27
Excess R_2O_3						
Fe_2O_3	—	—	—	3·02	5·85	11·07
Al_2O_3	—	—	—	—	0·04	—
	—	—	—	3·02	5·89	11·07

to the ideal value of 24. Titanomagnetites ST.40, ST.12, and ST.11 have cation totals less than 24, and are cation deficient γ-spinels lying on the $FeTiO_3$–Fe_2O_3 side of the Fe_2TiO_4–Fe_3O_4 join (fig. 4).

Unit-cell measurements were made in two ways. (1) By measurement of high-angle back reflections (showing $K\alpha_1$ and $K\alpha_2$ doublets) on powder photos taken on a 114·6 mm camera (Co/Fe radiation). (2) By repeated scanning of the (333, 511) spinel peak, using a Philips diffractometer (Co/Fe radiation), with quartz as an internal standard (cf. Lindsley,

1962). The adopted cell dimensions are considered accurate to at least $\pm 0{\cdot}002$ Å.

All the titanomagnetites have cell edges greater than the cell edge of stoichiometric natural Fe_3O_4, namely 8·396 Å (Basta, 1957). The recalculated normative compositions of titanomagnetites ST. 28, ST.20,

TABLE III. Chemical analyses of titaniferous magnetites

Analysis no.	1	2	3	4	5	6	7
FeO	50·13	29·74	46·06	45·22	42·33	33·79	29·79
MgO	2·04	n.d.	2·29	1·93	2·07	1·49	2·74
MnO	0·68	0·70	0·33	0·61	0·72	0·28	0·32
CaO	0·16	n.d.	0·06	0·59	—	0·20	1·30
Fe_2O_3	18·28	59·56	28·37	21·10	26·88	51·68	47·27
Al_2O_3	2·39	tr.	1·39	2·31	0·40	2·91	1·28
TiO_2	25·65	8·71	19·42	26·76	24·86	9·36	9·58
SiO_2	0·20	0·63	0·10	0·33	2·64	0·05	6·22
Etc.	—	—	2·04	0·75	—	0·71	0·31
Total	99·53	99·34	100·06	99·60	99·90	100·47	98·81
a (Å)	8·493	8·408	8·450	8·48	8·469	—	—
Recalculated normative compositions							
Magnetite, etc.	30·40	70·66	45·92	34·66	40·51	79·71	79·12
Ulvöspinel, etc.	66·00	—	53·43	43·80	32·30	8·72	—
Ilmenite, etc.	3·60	18·27	—	21·07	27·19	11·57	20·76
excess R_2O_3	—	11·07	—	—	—	—	—
excess MO	—	—	0·65	—	—	—	—
excess TO_2	—	—	—	—	—	—	0·06

1. Titanomagnetite from analcime–olivine theralite, Square Top intrusion (table 1, analysis 1).
2. Titanomagnetite from analcime–tinguaite, Square Top intrusion (table 1, analysis 6).
3. Magnetite–ulvöspinel intergrowth, lower olivine-gabbro (2308), Skaergaard intrusion, East Greenland. (Vincent *et al.*, 1957).
4. Titanomagnetite from teschenite, 20 feet above lower contact, Black Jack sill, Gunnedah, New South Wales (Wilkinson, 1957).
5. Titanomagnetite from basalt (S. 729), Giant's Causeway, Ireland (Basta, 1960).
6. Titaniferous magnetite from anorthosite, Schmoo Lake, near Lac la Blache, Comte du Saguenay, Quebec, Canada (Vincent *et al.*, 1957).
7. Titaniferous magnetite (ilmenite–magnetite intergrowths) from essexite (S. 461), Tofetholine, Oslo Fjord, Norway (Basta, 1960).

and ST.23 (table II) indicate significant amounts of the spinel Fe_2TiO_4 end-member. When these three minerals are considered solely in terms of Fe_3O_4–Fe_2TiO_4 end-members (mol. per cent.), their respective cell dimensions plot close to the curves relating composition and cell dimensions in the synthetic Fe_3O_4–Fe_2TiO_4 series (Akimoto *et al.*, 1957; Lindsley, 1962). The recalculated compositions of titanomagnetites

ST.40, ST.12, and ST.11 yield only Fe_3O_4, $FeTiO_3$, and Fe_2O_3 as the principal components.

The titanomagnetite powder photos show well-defined spinel lines; the strongest reflections of ilmenite (d = 2·75), γ-Fe_2O_3 (d = 2·51), and α-Fe_2O_3 (d = 2·69) are absent. The sharp diffractometer trace of the (333, 511) peak (scan speed $\frac{1}{4}°$/min) confirms the homogeneity of titanomagnetites ST.28, ST.20, and ST.23 in relation to a possible exsolved Fe_2TiO_4-rich spinel phase.

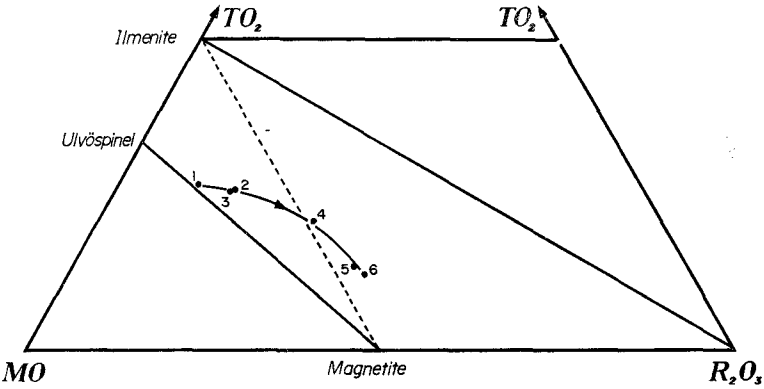

FIG. 1. Molecular compositions and course of crystallization of titanomagnetites from the Square Top intrusion. MO = FeO+MnO+MgO+CaO; R_2O_3 = Fe_2O_3 + Al_2O_3; TO_2 = TiO_2 + SiO_2. The numbers refer to analyses in table I.

General discussion

When the titanomagnetite analyses are plotted in terms of molecular proportions of MO, R_2O_3, and TO_2, their course of crystallization extends from close to the binary ulvöspinel–magnetite join, and near to ulvöspinel, towards magnetite, the Fe_2TiO_4-free variants lying in the field defined by ilmenite–magnetite–R_2O_3 (fig. 1). The regular titanomagnetite variation in FeO, Fe_2O_3, and TiO_2 is indicated by fig. 2 where these oxides are plotted against the differentiation index (D.I. = normative Ab+Or+Ne) of the parent rock (Thornton and Tuttle, 1960).

The Square Top titanomagnetite differentiation trend covers the range of composition indicated by the majority of TiO_2-bearing magnetites plotted by Akimoto (1954, 1955), Vincent *et al.* (1957), Basta (1960), and Nagata (1962). The trend in fig. 1 is opposite to the slope of the liquidus surface in the spinel field in the synthetic $FeO.Fe_2O_3.TiO_2$ system (Taylor, 1963), namely from Fe_3O_4 (m. pt. 1594° C) to Fe_2TiO_4

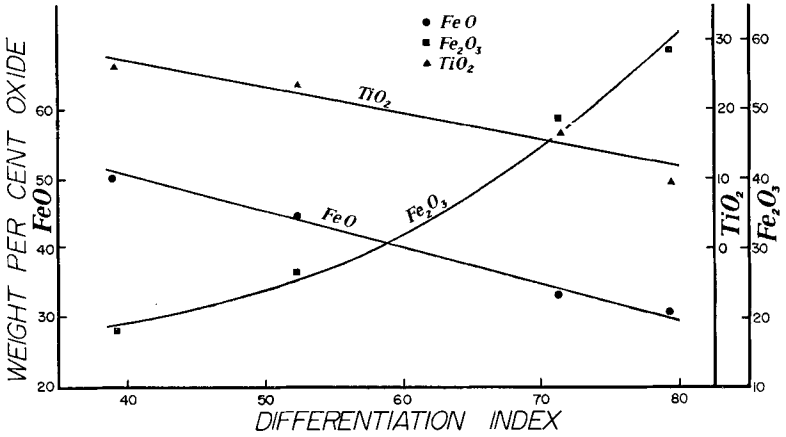

FIG. 2. Variation of titanomagnetite FeO, Fe_2O_3, and TiO_2 with differentiation of the parent rocks.

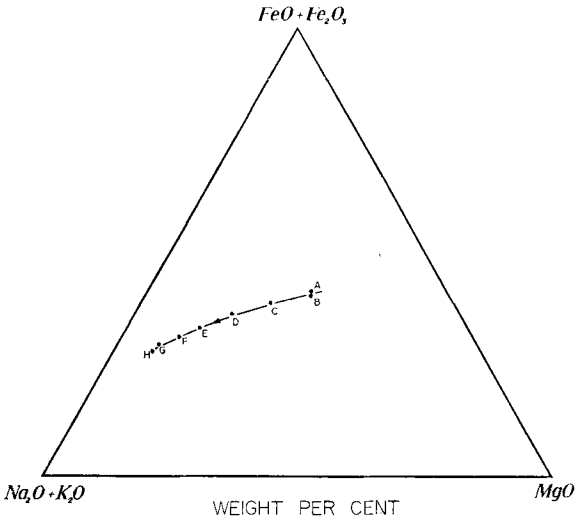

FIG. 3. Course of crystallization of rocks from the Square Top intrusion.

(m. pt. 1395° C). However, it should be stressed that although referable to the $FeO.Fe_2O_3.TiO_2$ system the titanomagnetites have crystallized from a sub-system within a more complex system in which alkali enrichment predominated over iron enrichment (fig. 3), the rock series trending with differentiation towards the low temperature area in the Ab Or–Ne–Ks quadrilateral. This course of parent rock crystallization

differs markedly from the Skaergaard reduced trend and from the majority of alkali olivine-basalt series studied by Nockolds and Allen (1954), where more pronounced relative iron enrichment takes place

TABLE IV. Chemical analyses of rocks from the Square Top intrusion

Analysis no.	1	2	3	4
Sample no.	ST.28	ST.20	ST.40	ST.12
Weight per cent.				
SiO_2	44·90	47·16	50·60	52·61
TiO_2	2·13	1·60	0·78	0·38
Al_2O_3	14·97	15·87	17·85	18·88
Fe_2O_3	2·62	3·33	4·11	4·06
FeO	8·26	6·05	3·13	1·72
MnO	0·15	0·14	0·13	0·11
MgO	8·45	6·15	3·13	1·62
CaO	9·08	7·01	3·87	2·43
Na_2O	5·02	6·42	8·03	8·93
K_2O	1·72	2·29	3·43	4·08
H_2O^+	1·21	2·57	2·95	3·72
H_2O^-	0·38	0·51	0·87	0·67
P_2O_5	0·97	0·94	0·78	0·55
Total	99·86	100·04	99·66	99·76
	Norms			
Or	10·01	13·34	20·02	24·46
Ab	13·10	21·48	31·96	32·49
An	13·34	8·06	2·78	—
Ne	15·90	17·61	19·31	22·44
Ac	—	—	—	1·39
Di	21·07	17·43	9·20	7·70
Ol	14·90	9·23	3·41	—
Mt	3·71	4·87	6·03	4·64
Hm	—	—	—	0·48
Il	3·95	3·04	1·52	0·76
Ap	2·35	2·02	2·02	1·34

1. Analcime–olivine theralite, close to lower western contact.
2. Leucocratic analcime–olivine theralite, on southern face approximately 70 feet above 1.
3. Melanocratic analcime–tinguaite, about 100 feet above lower eastern contact.
4. Analcime–tinguaite from exposed top of intrusion.

(Analyst M. Chiba.)

in the early stages of differentiation. The continued decrease of (Fe^{3+} + Fe^{2+}) with differentiation is referable to relatively high concentrations of water vapour, compared with many other intrusions, and mineralogically is expressed by increasing amounts of modal analcime. The values of H_2O^+ in the rock analyses in table IV may be noted. The close

relationship between titanomagnetite chemistry and the FeO, Fe_2O_3, and TiO_2 contents of the parent rocks is indicated by fig. 4.

The control of titanomagnetite composition by rock chemistry is considered more fundamental than any particular thermal trends present in the pure $FeO.Fe_2O_3.TiO_2$ system. This control may reverse trends of the gentle liquidi in the phase equilibria diagrams for Fe_2O_3 and Fe_3O_4, Fe_3O_4 and Fe_2TiO_4, $FeTiO_3$ and Fe_2TiO_4, and Fe_2O_3 and $FeTiO_3$ (Nagata, 1962).

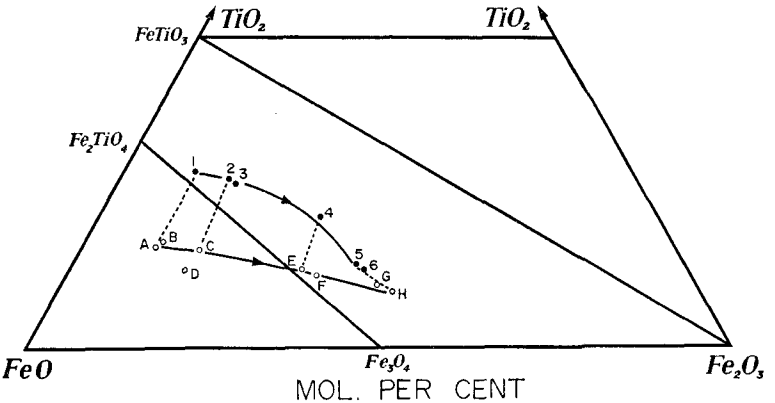

FIG. 4. Molecular compositions of the Square Top titanomagnetites (1–6) and rocks (*A–H*). The tie-lines (1–*A*, 2–*C*, 4–*E*, 5–*H*) link titanomagnetites and their respective parent rocks. Rocks *A–H* are the same as those plotted on fig. 3.

The data of Akimoto, Katsura, and Yoshida (1957) are important in considering the compositions and cell dimensions of the titanomagnetites. These workers oxidized synthetic titanomagnetites whose compositions originally lay along the Fe_2TiO_4–Fe_3O_4 join, delineating an area in the $FeTiO_3$–Fe_2TiO_4–Fe_3O_4–Fe_2O_3 field where the oxidized γ-titanomagnetites retained the spinel structure. The titanomagnetite compositions and their respective cell edges agree fairly closely with the relationships between cell dimensions and changing compositions of the synthetic titanomagnetites (Akimoto *et al.*, *op cit.*, fig. 6). Table V lists some comparative data in terms of molecular compositions and cell dimensions. X-ray measurements on additional material substantiate the trend of decreasing titanomagnetite cell dimensions with differentiation of the Square Top intrusion. Titanomagnetite from specimen ST.19 (point *D* in figs. 3 and 4) has $a = 8{\cdot}460$ Å, while for

titanomagnetite from specimen ST.18, approximately 50 feet above ST.19, a =8·456 Å.

A titanomagnetite from the top of the Black Jack sill (Wilkinson, 1957) may be noted in the light of these synthetic data. This mineral (FeO 44·3, Fe_2O_3 20·5, TiO_2 35·2 mol. %)[1] shows only spinel lines on

TABLE V. Compositions (mol. per cent.) and cell edges of titanomagnetites

Specimen	FeO	Fe_2O_3	TiO_2	a (Å)
ST.28	61·6	10·1	28·3	8·493
ST.20	57·5	15·2	27·3	8·477
ST.40	47·7	31·3	21·0	8·429
ST.12	46·8	40·0	13·2	8·410
ST.11	46·2	41·6	12·2	8·408
S2–7	58·93	14·53	26·54	8·486
S2–6	59·73	17·55	22·72	8·473
S2–6′	40·77	33·58	25·65	8·417
S2–4′	40·80	40·89	18·31	8·404

Data on S2–7 to S2–4′ from Akimoto *et al.*, 1957.

a powder photo; a = 8·42 Å. When all the TiO_2 is allotted initially to $FeTiO_3$, the chemical analysis shows excess Fe_2O_3. An oxidized synthetic titanomagnetite (S5–6′; FeO 43·54, Fe_2O_3 22·74, TiO_2 33·72 mol. %) prepared by Akimoto *et al.* retained the spinel structure; a = 8·423 Å.

The homogeneity of the Square Top titanomagnetites accords with the coexisting silicates in indicating a rate of cooling of the intrusion comparable to volcanic rocks of similar composition. In the case of the Fe_2TiO_4-bearing titanomagnetites ST. 28, ST. 20, and ST.23, their rate of cooling below 600° C (the crest of the Fe_3O_4–Fe_2TiO_4 solvus; Kawai, 1959) was sufficiently rapid to prevent any unmixing.

Plagioclases ST.28 and ST.20 (An/(Ab+An) wt % = 55·5 and 46·1 respectively) possess a structural state more appropriate to high-temperature plagioclase, indicated by measurements of Γ (= 2θ (131)+ 2θ (220)—4θ ($1\bar{3}1$)) (Smith and Gay, 1958). The alkali feldspars (members of the low sanidine–high albite series) show slight evidence of submicroscopic unmixing; the lime-poor varieties are readily homogenized by heat treatment at 900° C for 24 hours. The nepheline phenocrysts in analcime–tinguaite ST.12 have the composition $Ne_{81}Ks_{12}Qz_7$, indicating a temperature of crystallization close to 700° C; the rock ST.12 plots in

[1] After allocation of CaO to form sphene.

the low temperature area in the as yet incompletely contoured Ab–Or–Ne–Ks quadrilateral, close to the 790° C isotherm determined at 15 000 psi water pressure (Hamilton, 1961).

Titanomagnetites ST.40, ST.12, and ST.11, whose recalculated compositions may be regarded in terms of Fe_3O_4–(γ-$FeTiO_3$)–(γ-Fe_2O_3) solid solutions, would presumably exsolve ferriilmenite or ilmenite and hematite under appropriate cooling conditions. There are data indicating negligible solid solution of ilmenite in magnetite at magmatic temperatures (Basta, 1960; Verhoogen, 1962; Lindsley, 1962), certainly in amounts too small tc explain the amounts of exsolved ilmenite in natural magnetite–ilmenite intergrowths. These intergrowths are often interpreted in terms of the oxidation of Fe_2TiO_4–Fe_3O_4 solid solutions. Some difficulties in this interpretation have been emphasized by Buddington *et al.* (1963), particularly (1) whether it can be shown that all or most natural titaniferous magnetites lying near or on the Fe_3O_4–$FeTiO_3$ join initially did form as Fe_2TiO_4–Fe_3O_4 solid solutions; and (2) the mechanics by which the Fe_2TiO_4 in the titanomagnetite is assumed to be oxidized to $FeTiO_3$ in the sub-solidus state throughout large bodies of rock. Vincent (1960) has described the *sub-solvus* oxidation of ulvöspinel to ilmenite in certain Skaergaard gabbros.

It is difficult to prove whether the compositions of the γ-spinels ST.40, ST.12, and ST.11 reflect the amounts of Fe^{3+}, Fe^{2+}, and Ti^{4+} available in a particular liquid fraction or whether they now represent oxidation products of β-spinels originally lying on the Fe_2TiO_4–Fe_3O_4 join. In terms of compositions and degree of oxidation these titanomagnetites represent spinels transitional to titanomaghemite. The latter mineral has been observed *developing* as an oxidation product along margins and cracks in original titanomagnetite (Katsura and Kushiro, 1961).

It is considered that the comparatively oxidized nature of some of the Square Top titanomagnetites primarily reflects their response to the varying compositions of successive liquid fractions. With differentiation, modal olivine, clinopyroxene, and titanomagnetite decrease. These relations are expressed chemically by progressively decreasing ($FeO+Fe_2O_3$) and MgO values in the parent rocks. In fig. 4, the rock differentiation trend, displaced from FeO towards Fe_2O_3, reflects the modal trends of the mafic minerals and increasing iron oxidation. In the theralites, $FeO > Fe_2O_3$, but with differentiation this relationship is reversed. On available chemical data this reversal occurs at a stage of differentiation somewhere between rocks *D* and *E* in fig. 3. The

clinopyroxenes do not show any significant variation in their Fe^{2+}/Mg ratios; bulk olivine compositions, at least as far as specimen ST.18 (which would plot between *D* and *E* in fig. 3) also show comparatively limited Fa enrichment, despite decreasing amounts of modal olivine and magnesium in the melt.

These aspects of the mafic mineralogy are ascribed to increasing oxidation of Fe^{2+} during differentiation, consequent to increasing water-vapour pressure, a relation manifest in increasing amounts of modal analcime.

TABLE VI. Oxidation ratios $Fe^{3+}/(Fe^{2+}+Fe^{3+})$ of titanomagnetites, rocks, and clinopyroxenes

Specimen	Titanomagnetite	Rock	Clinopyroxene
ST.28	0·25	0·22	0·37
ST.20	0·35	0·33	—
ST.40	0·57	0·54	—
ST.12	0·63	0·68	(i) mauve phenocrysts 0·45 (ii) pale green phenocrysts and ground-mass clinopyroxene 0·67
ST.11	0·64		pale green clinopyroxene 0·52

Table VI lists data indicating the degree of oxidation of the titanomagnetites, their parent rocks, and some coexisting clinopyroxenes. The ratio $Fe^{3+}/(Fe^{2+}+Fe^{3+})$ for the titanomagnetites is slightly greater than for the parent rock, a relation dependent primarily on the presence of modal olivine. Nevertheless, the titanomagnetite oxidation ratios do not depart significantly from the rock ratios, and in two instances are less than the ratios of coexisting clinopyroxene. On textural grounds the latter mineral always crystallized before the titanomagnetite. Although the amount of Fe^{3+} in the clinopyroxene to some degree reflects availability of Na for the $NaFe^{3+}$ Si_2O_6 end-member in solid solution, it nevertheless does indicate Fe^{3+}/Fe^{2+} relationships in the melt.

Presumably any possible sub-solidus oxidation is related to the interval between initial precipitation of the titanomagnetite and the final consolidation of the parent rock. The evidence indicating rapid cooling of the Square Top intrusion is re-emphasized. It may be noted also that titanomagnetite ST.28 from the lower levels of the intrusion is still preserved as essentially a Fe_2TiO_4–Fe_3O_4 solid solution, although it possessed the opportunity to undergo oxidation subsequent to its crystallization.

The excess Fe_2O_3 indicated by the recalculated compositions of ST.40, ST.12, and ST.11 is considered to be present as γ-Fe_2O_3 in solid solution. The X-ray and microscopic data indicate either the absence or only trace amounts of Fe_2O_3 as a separate phase.

In many rock series TiO_2 decreases with differentiation. Hence possible Fe_2TiO_4–Fe_3O_4 solid solutions trend towards Fe_3O_4 with falling temperature. The assumption that the original spinels originally lay along the ulvöspinel–magnetite join requires a continued delicate balance between Fe^{2+} and Fe^{3+} in the parent melts, and for spinels with significant amounts of Fe_2TiO_4, more or less continuous reducing conditions. Such conditions would not be expected to occur in many differentiated intrusions.

While acknowledging the hypothetical nature of γ-$FeTiO_3$, the writer considers that, although some magnetite–ilmenite intergrowths may result from the oxidation of Fe_2TiO_4–Fe_3O_4 solid solutions, many intergrowths of this type are developed from the exsolution and inversion of $FeTiO_3$ from Fe_2TiO_4–Fe_3O_4–(γ-$FeTiO_3$) or Fe_3O_4–(γ-$FeTiO_3$) solid solutions, particularly those iron-titanium oxides from many differentiated intrusions. The latter view is favoured by Nicholls (1955), Basta (1960), and Vincent (1960).

Acknowledgements. This study was assisted by a Research Grant from the University of New England. The writer thanks S. E. Shaw for carrying out additional duplicate analytical determinations of certain titanomagnetite constituents.

References

Akimoto (S.), 1954. Journ. Geomagn. Geoelectr., vol. 6, no. 1, p. 1.
—— 1955. Japan Journ. Geophys., vol. 1, no. 2, p. 1.
—— Katsura (T.), and Yoshida (M.), 1957. Journ. Geomagn. Geoelectr., vol. 9, no. 4, p. 165.
Basta (E. Z.), 1957. Min. Mag., vol. 31, p. 431.
—— 1960. Neues Jahrb. Min. Abh., vol. 94, p. 1017. (Festband Ramdohr).
Buddington (A. F.), Fahey (J.), and Vlisidis (A.), 1955. Amer. Journ. Sci., vol. 253, p. 497.
—— —— —— 1963. Journ. Petrology, vol. 4, p. 138.
Hamilton (D. L.), 1961. Journ. Geol., vol. 69, p. 321.
Katsura (T.) and Kushiro (I.), 1961. Amer. Min., vol. 46, p. 134.
Kawai (N.), 1959. 20th Int. Geol. Congr., 11–A, p. 103.
Lindsley (D. H.), 1962. Carnegie Yearb. 61, p. 100.
Nagata (T.), 1962. Proc. Benedum Earth Magn. Symp., p. 69.
Nicholls (G. D.), 1955. Phil. Mag., suppl., vol. 4, p. 113.
Nockolds (S. R.) and Allen (R.), 1954. Geochimica Acta, vol. 5, p. 245.
Smith (J. V.) and Gay (P.), 1958. Min. Mag., vol. 31, p. 744.
Taylor (R. W.), 1963. Journ. Amer. Ceramic Soc., vol. 46, p. 276.
Thornton (C. P.) and Tuttle (O. F.), 1960. Amer. Journ. Sci., vol. 258, p. 664.

VERHOOGEN (J.), 1962. Journ. Geol., vol. 70, p. 168.
VINCENT (E. A.), 1960. Neues Jahrb. Min. Abh., vol. 94, p. 993 (Festband Ramdohr).
—— and PHILLIPS (R.), 1954. Geochimica Acta, vol. 6, p. 1.
—— WRIGHT (J. B.), CHEVALLIER (R.), and MATHIEU (S.), 1957. Min. Mag., vol. 31, p. 624.
WILKINSON (J. F. G.), 1957. Min. Mag., vol. 31, p. 443.